

# REDUCED-EMITTANCE LATTICE FOR AmPS

G. Luijkx and R. Maas, NIKHEF, P.O. Box 41882, 1009 DB Amsterdam, The Netherlands.

## Abstract

AmPS is a 900 MeV electron ring [1–3]. The machine comprises 4 Curved Sections (21 m ea.), connected by long (32 m ea.) dispersion-free Straight Sections. AmPS had been originally designed as a Pulse Stretcher, using the extracted beam as a nearly continuous electron source for carrying out (mainly) coincidence electron scattering studies in sub-atomic physics. Gradually the internal (stored) beam is also used for fundamental physics research. The original 2856 MHz RF-system has been supplemented by a 476 MHz RF-system, allowing storage of beams at energies up to 1 GeV. In the Storage Mode option users are interested in beams with a smaller emittance than provided when using the original Stretcher lattice. For this reason an additional reduced-emittance (RE) lattice configuration has been developed, in which the emittance is reduced by a factor of three. This has been accomplished by converting the four-cell structure of the Curves into two achromats. Since the magnet layout remains unchanged in the RE-configuration, the original Stretcher operation remains available.

## 1 EMITTANCE

The (horizontal) emittance  $\varepsilon_x$  is basically a lattice parameter with a quadratic dependence on the energy:

$$\varepsilon_x = \frac{55}{32\sqrt{3}} \frac{h}{m_0c} \gamma^2 \frac{I_5}{I_2 - I_4} \quad (1)$$

The lattice properties enter by the *synchrotron integrals*  $I_n$ ;  $\gamma$  is the Lorentz factor.

$$I_2 = \oint \frac{1}{\rho^2(s)} ds \quad (2)$$

$\rho$  is the bending radius of the dipoles (AmPS:  $\rho = 3.3$  m). Since  $\rho(s) = \rho$ , (2) can be evaluated as  $I_2 = 2\pi/\rho = 1.9$   $m^{-1}$ . So for a given value of  $\rho$  the value of  $I_2$  is fixed.  $I_4$  for rectangular magnets can be shown [4] to be

$$I_4 = N \frac{2}{\rho} [\varphi / 2 - \tan(\varphi / 2)]$$

$N$  is number of dipoles,  $\varphi$  is bending angle. For AmPS  $I_4 = -0.006$   $m^{-1}$  so  $I_4$  is of no concern here.

$$I_5 = \oint \frac{H(s)}{|\rho^3(s)} ds \quad (3)$$

with

$$H(s) = \frac{1}{\beta(s)} \left[ \eta^2(s) + \left\{ \beta(s)\eta'(s) - \frac{1}{2}\beta'(s)\eta(s) \right\}^2 \right]$$

$\eta$  is the dispersion function. (3) indicates that contributions to  $I_5$  are proportional to the value of  $\eta^2$  inside the dipoles (using the approximation from [5])

$$\eta(s) \approx \left( \frac{\alpha R}{v_x} \right)^{1/2} \beta^{1/2}(s)$$

it follows that the expression between curly brackets vanishes.  $R$  is the gross-radius of machine).

Since  $\varepsilon_x$  depends linearly on  $I_5$ , the recipe for a small emittance is clear:

*design a lattice in which the dispersion function  $\eta$  inside the dipoles is small.*

The properties of the Straight Sections are irrelevant for the value of the emittance.

For the present AmPS lattice:  $I_5 = 0.26$   $m^{-1}$ . Putting this value and the one for  $I_2$  into (1) yields:

$$\varepsilon_x = 159 \text{ nm.rad @ 900 MeV}$$

## 2 REDUCED EMITTANCE CONFIGURATION

The structure of the present Curved Sections is given in Fig. 1. It is a four-fold symmetric structure. The ('half') end-quads are connected to similar 'half' quads of the connecting Straight Sections, forming thus a full-length quad. So each curve comprises 5  $q_h$  and 4  $q_v$  quads. These quads are powered in series (including the quads of the other three Curves), so two power supplies are required to power all the quads in the Curves.

The chromaticity is controlled by two families of sextupoles: horizontally/vertically-focusing sextupoles are indicated by  $s_h$  and  $s_v$  respectively, see Fig.1 .

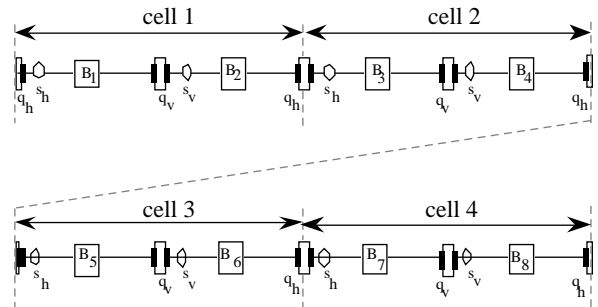


Fig.1 Structure of the present Curve. B is dipole, q is quadrupole, s is sextupole; subscripts h and v indicate horizontal and vertical respectively.

Machine functions ( $\beta_x$ ,  $\beta_y$  and  $10 \times \eta$ ) of this structure are given in Fig.2 ('Stretcher lattice'). It can be observed that especially in the four centre dipoles  $B_3 - B_6$  the  $\eta$ -function is large (1 à 1.5 m).

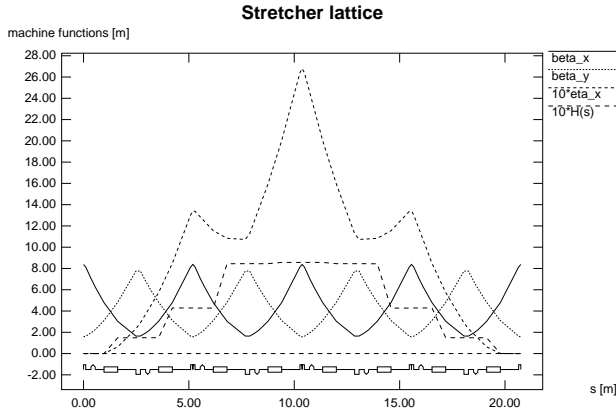


Fig.2 Machine functions in the Curves in the original Stretcher-lattice configuration.

Fig.3 shows the structure of the RE-lattice; it has a two-fold symmetric structure, but maintains the same basic component layout as the original Curve of Fig.1. The, different powering of the quads results in a lower emittance, see below.

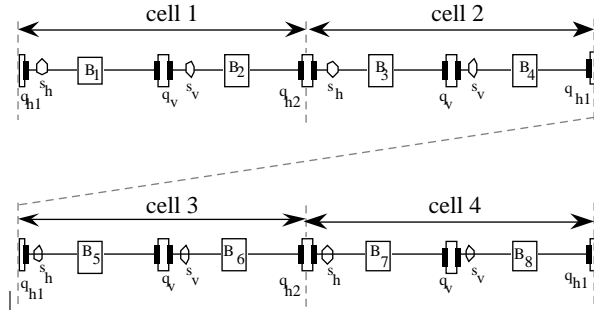


Fig.3 Structure of Curve in 'reduced lattice'-configuration. Structure (cell 1-cell 2) is repeated as (cell 3-cell 4). Three different quadrupoles are used:  $q_{h1}$ ,  $q_v$  and  $q_{h2}$ . Sextupoles are indicated by  $s_h$  (hor.) and  $s_v$  (vert.).

Quad  $q_{h1}$  is 'shared' with the first quad of the connecting straight section, so the complete Curve consists of  $3 \times q_{h1}$ ,  $4 \times q_v$  and  $2 \times q_{h2}$ .

Consequently, one additional power supply will be needed to power all the quads in the Curves

Machine functions ( $\beta_x$ ,  $\beta_y$  and  $10 \times \eta$ ) of this structure are given in Fig.4 ('reduced emittance'). Comparison with Fig.2 shows a substantial reduction of the integral value of  $\eta$  over the dipoles, which is the basis of the emittance reduction by a factor of three compared to the original optics.

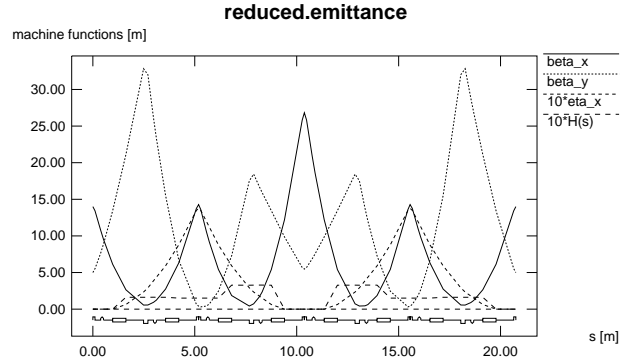


Fig.4 Machine functions in the Curves in the reduced-emittance configuration. Comparison with Fig.2 shows a substantial reduction of the  $\eta$ -function.

### 3 MACHINE PARAMETERS

In Table 1 a comparison is made between machine parameters (and some related data) of the original Stretcher lattice and the proposed reduced-emittance configuration for  $E = 900$  MeV. It should be noted that in the RE-configuration both  $\alpha_x$  and  $\alpha_y$  are  $\neq 0$  at the beginning and end of each Curve. Since the connecting Straight Sections comprise two parts connected mirror-symmetrically, no mismatch will occur, see Sect. 6.

Table 1. Comparison between machine properties of 'reduced-emittance'-lattice and original 'Stretcher lattice'. The chromaticity sextupoles are  $s_h$  and  $s_v$ .

machine properties		reduced-emittance lattice	original lattice
energy	MeV	900	900
emittance $\epsilon_x$	nm.rad	49	159
momentum compaction $\alpha$		0.011	0.027
horizontal tune $\nu_x$		11.22	8.30/8.43
vertical tune $\nu_y$		7.83	7.19
energy spread $\sigma_E$	%	0.043	0.043
damp. time $\tau_x$	ms	72	72
natural chromaticity $\chi_x$		-22.3	-9.4
natural chromaticity $\chi_y$		-21.3	-9.5
$\beta_x$ (start/end of Curve)	m	14.0	8.0
$\beta_y$ (start/end of Curve)	m	5.0	1.6
$\alpha_x$ (start/end of Curve)		0.225	0.0
$\alpha_y$ (start/end of Curve)		-1.5	0.0
<b>tip fields</b>			
$q_{h1}$	kG	3.57	2.75
$q_v$	kG	-2.87	-2.53
$q_{h2}$	kG	3.97	
$s_h$ (@ $\chi_x = +0.2$ )	kG	0.53	0.17
$s_v$ (@ $\chi_y = +0.2$ )	kG	-0.55	-0.28

## 4 STRAIGHT SECTIONS

The Straight Sections are basically identical; the Injection Straight differs slightly from the other ones due to the additional constraint of the required 180° phase difference between the two injection kickers. Each Straight comprises two identical parts (containing 4 'full' quads, and a 'half' quad, which connects to an end 'half' quad of a Curve), joined 'back-to-back'.

## 5 CHROMATICITY AND TUNE

The chromaticity can be expressed in machine parameters as

$$\chi_z = -\frac{1}{4\pi} \oint K_z(s) \beta_z(s) ds, \quad z = x, y$$

Since in the RE-configuration both the quadrupole strengths and the  $\beta$ -functions in the Curves have increased compared to the Stretcher lattice, the natural chromaticity will be increased, see Table 1. Since the *location* of the sextupoles in the RE-lattice is still very functional (i.e. the x-sextupole is still located where  $\beta_x$  is large and  $\beta_y$  is small, and vice versa), an efficient parametrisation of the chromaticity control could be defined.

Tune control is accomplished by four families of quads in three Straight Sections. Two degrees of freedom are used to control both  $\nu_x$  and  $\nu_y$ ; the two remaining ones keep both  $\alpha_x$  and  $\nu_y$  zero at the symmetry point in the Straights. Changing the tune, therefore, hardly affects the optics. The Injection Straight is not included in the tune control in order to maintain the 180° phase difference between the two injection kickers as accurate as possible.

## 6 MATCHING

A schematic layout of AmPS is given in Fig. 5:

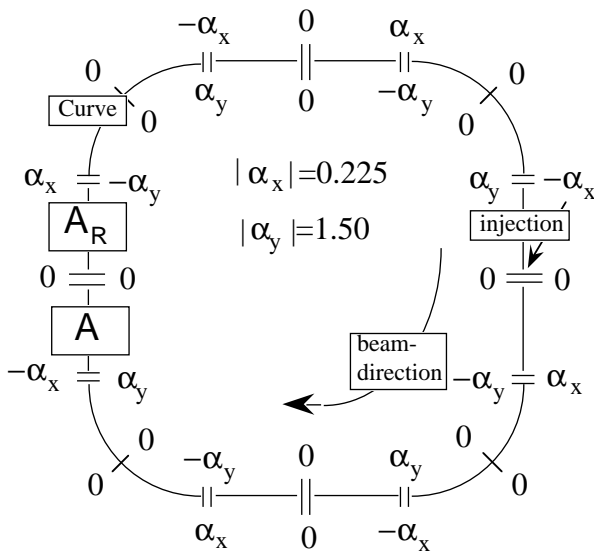
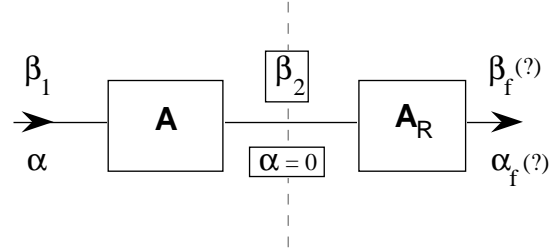


Fig.5 Schematic layout of AmPS ring. The values of both  $\alpha_x$  and  $\alpha_y$  are given at the positions where Curves and Straights connect.

The matrices of the two modules which make the West Straight are indicated by A and  $A_R$ , with  $A_R$  being the reflected transform of A [6]:

$$A = \begin{pmatrix} r_{11} & r_{12} \\ r_{21} & r_{22} \end{pmatrix}; \quad A_R = \begin{pmatrix} r_{22} & r_{12} \\ r_{21} & r_{11} \end{pmatrix}$$

The system can now be visualised as:



Calculating both  $\beta_f$  and  $\alpha_f$  for  $A_R$  with initial conditions  $\beta_i = \beta_2$  and constraint  $\alpha_i = 0$ , one finds

$$\alpha_f = -\alpha \text{ and } \beta_f = \beta_1.$$

This property is true for both transverse planes.

A similar situation exists in the Curves: also there exists a mirror-symmetry around the centre of the structure, and at this centre  $\alpha_x = \alpha_y = 0$ .

## 7 IMPLEMENTATION

The implementation of the RE-mode consisted of adding an additional quadrupole power supply and installing new protocols for machine control, tune and chromaticity. Also new powersupplies for the chromaticity sextupoles were installed. The implementation did not involve relocation of magnets other than a few small steering magnets to facilitate the creation of local bumps. The RE-configuration will be commissioned late June, 1996. A very preliminary test indicated beam storage at this new configuration, but no real measurements have been performed yet.

## REFERENCES

- [1] R. Maas and Y. Wu, 'Optics of the Amsterdam Pulse Stretcher, Proc. 1989 IEEE Part. Accel. Conf., p. 1698, 1989
- [2] G. Luijckx et al., 'The Amsterdam Pulse Stretcher Project (AmPS), Proc. 1989 IEEE Part. Accel. Conf., p. 46, 1989
- [3] R. Maas et al., 'Commissioning results of the Amsterdam Pulse Stretcher/Storage Ring AmPS', Proc. 1993 IEEE Part. Accel. Conf., p. 1998, 1993
- [4] J.A. Uythoven et al., 1st European Part. Accel. Conf., Rome, June 7-11, 1988, pp. 649-650.
- [5] M. Sands, 'The Physics of Electron Storage Rings. An Introduction', SLAC-121 (1970).
- [6] S. Penner, 'Calculations of Properties of Magnetic Deflection Systems', Rev. Sci. Instr., vol.32, nr.2, pp.150-160, 1961.